Antiferromagnetic Phases in the Fulde-Ferrell-Larkin-Ovchinnikov State of $CeCoIn_5$

Youichi YANASE[1,2*] and Manfred Sigrist[2]

[1]*Department of Physics, Niigata University, Ikarashi, Niigata 950-2181, Japan*
[2]*Theoretische Physik, ETH-Honggerberg, 8093 Zurich, Switzerland*

(Received Today 2010)

The antiferromagnetic (AFM) order in the Fulde-Ferrell-Larkin-Ovchinnikov (FFLO) superconducting state is analyzed on the basis of a Ginzburg-Landau theory. To examine the possible AFM-FFLO state in $CeCoIn_5$, we focus on the incommensurate AFM order characterized by the wave vector $\vec{Q} = \vec{Q}_0 \pm \vec{q}_{\rm inc}$ with $\vec{Q}_0 = (\pi, \pi, \pi)$ and $\vec{q}_{\rm inc} \parallel [110]$ or $[1\bar{1}0]$ in the tetragonal crystal structure. We formulate the two component Ginzburg-Landau theory and investigate the two degenerate incommensurate AFM order with $\vec{q}_{\rm inc} \parallel [110]$ and $[1\bar{1}0]$. We show that the pinning of AFM moment due to the FFLO nodal planes leads to multiple phases in magnetic fields along [100] or [010]. The phase diagrams for various coupling constants between the two order parameters are shown for the comparison with $CeCoIn_5$. Experimental results of the NMR and neutron scattering measurements are discussed.

KEYWORDS: FFLO superconductivity, unconventional magnetism, $CeCoIn_5$

1. Introduction

The possible presence of a spatially modulated state in spin polarized superconductors was predicted by Fulde and Ferrell,[1)] and by Larkin and Ovchinnikov[2)] more than 40 years ago. While the Bardeen-Cooper-Schrieffer (BCS) theory assumes Cooper pairs with vanishing total momentum, the FFLO superconducting state represents a condensate of Cooper pairs with a finite total momentum. Since the FFLO state has an internal degree of freedom arising from the reflection or inversion symmetry, a spontaneous breaking of the spatial symmetry occurs.

Although this novel superconducting state with an exotic symmetry has been attracting much interest, the FFLO state has not been observed in superconductors for nearly 40 years. Naturally, the discovery of a new superconducting phase in $CeCoIn_5$ at high magnetic fields and low temperatures[3,4)] triggered numerous theoretical and experimental studies because this high-field superconducting (HFSC) phase is a most likely candidate for the FFLO state.[5)] The recent interest on the FFLO superconductivity/superfluidity extends further into various related fields, such as organic superconductors,[6–9)] cold atom gases,[10,11)] astrophysics, and nuclear physics.[12)]

Although the HFSC phase of $CeCoIn_5$ has been interpreted widely within the concept of the FFLO state,[5,13–21)] recent observations of the magnetic order in the HFSC phase call for a reexamination of this conclusion.[22,23)] Neutron scattering measurements have shown that the wave vector of the AFM order is incommensurate $\vec{Q} = \vec{Q}_0 \pm \vec{q}_{\rm inc}$ with $\vec{Q}_0 = (\pi, \pi, \pi)$ and the incommensurate wave vector is fixed to $\vec{q}_{\rm inc} \sim (0.12\pi, \pm 0.12\pi, 0)$ independent of the orientation of magnetic field.[23,24)] The AFM staggered moment $\vec{M}_{\rm AF}$ lies along the c-axis.[23,24)] For the magnetic field along [110] direction, the incommensurate wave vector is perpendicular to the magnetic field $\vec{q}_{\rm inc} \sim (0.12\pi, -0.12\pi, 0)$, while the two degenerate incommensurate AFM states with $\vec{q}_{\rm inc} \sim (0.12\pi, 0.12\pi, 0)$ and $\vec{q}_{\rm inc} \sim (0.12\pi, -0.12\pi, 0)$ appear in the magnetic field along [100] direction.[23,24)]

The magnetic order of $CeCoIn_5$ appears in the superconducting state, but not in the normal state. This coupling between the magnetism and superconductivity is in sharp contrast to the other heavy fermion superconductors where the magnetic order is suppressed by superconductivity.[25)] Another important feature of $CeCoIn_5$ is the enhancement of HFSC phase under pressure.[17)] This feature is also in contrast to conventional magnetic order in Ce-based heavy fermion systems which is suppressed by pressure.[25)] These unusual features indicate that the magnetic order of $CeCoIn_5$ is not a conventional AFM order.

Several intriguing quantum phases have been theoretically proposed for the unconventional magnetic order in $CeCoIn_5$.[26–32)] Our proposal is based on the presence of AFM quantum critical point near the superconducting phase of $CeCoIn_5$.[33,34)] We have shown that the AFM order occurs when the inhomogeneous Larkin-Ovchinnikov state is stabilized in the vicinity of the AFM quantum critical point.[26,27)] The coupling between the magnetism and FFLO superconductivity seems to be consistent with the above-mentioned unusual feature that the magnetically ordered phase is confined in the superconducting phase in the H-T phase diagram.[22,23)] Another proposal has been given on the basis of the emergence of a pair density wave state.[29–31)]

In order to identify the HFSC phase of $CeCoIn_5$ it is highly desirable to investigate these proposed phases for a comparison with experimental results. For this purpose, we investigate the AFM phases in the FFLO state. We show that the multiple phases appear in the AFM-FFLO state when the magnetic field is applied along [100] or [010] direction. We discuss the possible phase diagram of $CeCoIn_5$ on the basis of the comparison with experiments.

2. Formulation

An intriguing magnetic phase diagram arises from the degeneracy between the incommensurate wave vector

$\vec{q}_{\rm inc} \sim (0.12\pi, 0.12\pi, 0)$ and $\vec{q}_{\rm inc} \sim (-0.12\pi, 0.12\pi, 0)$ in the magnetic field along [100] or [010] direction. In order to investigate the magnetic phases, we formulate the phenomenological two component Ginzburg-Landau model. We here consider the AFM order in the inhomogeneous Larkin-Ovchinnikov state for which the Ginzburg-Landau functional of the free energy is described as,

$$\begin{aligned} F(\eta_1,\eta_2)/F_0 = & [(T/T_{\rm N}^0 - 1) + \xi_{\rm AF}^2(\vec{q}_1 - \vec{q}_{\rm inc}^{(1)})^2]\eta_1^2 \\ & + [(T/T_{\rm N}^0 - 1) + \xi_{\rm AF}^2(\vec{q}_2 - \vec{q}_{\rm inc}^{(2)})^2]\eta_2^2 \\ & + \frac{1}{2}(\eta_1^2+\eta_2^2)^2 + b\eta_1^2\eta_2^2 + c_1 H_{\rm x} H_{\rm y}(\eta_1^2 - \eta_2^2) \\ & - \frac{1}{2}\eta_1\eta_2 \sum_n c_2(n)\delta(\vec{q}_1 - \vec{q}_2, 2n\vec{q}_{\rm FFLO}), \quad (1) \end{aligned}$$

where η_1 and η_2 are the two component order parameters corresponding to the two degenerate AFM states with $\vec{Q} = \vec{Q}_0 \pm \vec{q}_1 \sim \vec{Q}_0 \pm \vec{q}_{\rm inc}^{(1)}$ and $\vec{Q} = \vec{Q}_0 \pm \vec{q}_2 \sim \vec{Q}_0 \pm \vec{q}_{\rm inc}^{(2)}$, respectively. The wave vector of incommensurate AFM order is assumed as $\vec{q}_{\rm inc}^{(1)} = (0.125\pi, 0.125\pi, 0)$ and $\vec{q}_{\rm inc}^{(2)} = (-0.125\pi, 0.125\pi, 0)$. Small deviations of wave vectors from $\vec{q}_{\rm inc}^{(1)}$ and $\vec{q}_{\rm inc}^{(2)}$ due to the pinning of FFLO nodal planes are taken into account in eq.(1). In our study the incommensurate wave vectors $\vec{q}_{\rm inc}^{(1)}$ and $\vec{q}_{\rm inc}^{(2)}$ are not microscopically derived but assumed on the basis of the experimental results in Refs. 23 and 24. We think that the $\vec{q}_{\rm inc}^{(1)}$ and $\vec{q}_{\rm inc}^{(2)}$ are pinned through nesting features in the band structures.

We define the AFM staggered moment $M_{\rm AF}(\vec{r}) = (-1)^{x+y+z}M(\vec{r})$ where $M(\vec{r})$ is the magnetic moment perpendicular to the applied magnetic field at $\vec{r} = (x, y, z)$. Then, the AFM staggered moment is described as,

$$M_{\rm AF}(\vec{r}) = M_0[\eta_1 \cos(\vec{q}_1 \cdot \vec{r}) + \eta_2 \cos(\vec{q}_2 \cdot \vec{r})], \quad (2)$$

where M_0 (and F_0) are scaling factors by which the Ginzburg-Landau free energy is written in the renormalized form (eq.(1)). We take the unit of magnetic moment and energy so that $M_0 = F_0 = 1$. The $T_{\rm N}^0$ is the Néel temperature for $c_1 = c_2(n) = 0$ and $\xi_{\rm AF}$ is the coherence length of AFM order.

The phase diagram of the Ginzburg-Landau model considerably depends on the sign of the non-linear quartic coupling term b. The single-q magnetic structure $(\eta_1, \eta_2) \propto (1, 0)$ or $(0, 1)$ is stabilized by the positive coupling constant b, while the negative b favors the double-q magnetic structure $(\eta_1, \eta_2) \propto (1, \pm 1)$.

The coupling constant c_1 describes the effect of magnetic field $\vec{H} = (H_{\rm x}, H_{\rm y}, H_{\rm z})$ which may break the degeneracy of η_1 and η_2. According to the neutron scattering measurement for $\vec{H} \parallel [110]$,[23] c_1 is positive in $CeCoIn_5$. This is consistent with our theoretical analysis based on the Bogoliubov-de-Gennes (BdG) equations.[26,27,35] When we consider the magnetic field along [100] direction, this term vanishes and therefore the degeneracy of η_1 and η_2 remains. We focus on this case in this paper.

Effects of the broken translation symmetry in the inhomogeneous Larkin-Ovchinnikov state are taken into account in the commensurate term, that is the last term of eq.(1). We define $\delta(\vec{q}_1 - \vec{q}_2, 2n\vec{q}_{\rm FFLO}) = 1$ when the commensurate condition $\vec{q}_1 - \vec{q}_2 = 2n\vec{q}_{\rm FFLO}$ is satisfied for an integer n, and otherwise $\delta(\vec{q}_1 - \vec{q}_2, 2n\vec{q}_{\rm FFLO}) = 0$. The modulation vector of FFLO state is denoted as $\vec{q}_{\rm FFLO}$, and then the order parameter of superconductivity is described as $\Delta(\vec{r}) = \Delta_0 \sin(\vec{q}_{\rm FFLO} \cdot \vec{r})$. The commensurate term describes the pinning effect of FFLO nodal planes for the AFM moment. According to our analysis based on the BdG equation, the AFM moment is enhanced around the FFLO nodal planes where the superconducting order parameter vanishes.[26,27,35] Then, we obtain the positive coupling constant $c_2(n) \geq 0$.

3. Magnetic Phases

We here consider the FFLO state in which the higher harmonic FFLO wave vector $2N\vec{q}_{\rm FFLO}$ is close to $\vec{q}_{\rm inc}^{(1)} - \vec{q}_{\rm inc}^{(2)}$. Then, the broken translation symmetry plays an important role for the appearance of magnetic phases as will be shown below. When the wave vector $\vec{q}_{\rm inc}^{(1)} - \vec{q}_{\rm inc}^{(2)}$ is not in the vicinity of $2n\vec{q}_{\rm FFLO}$ for any integer n, the commensurate term can be neglected. Then, the single-q magnetic phase with $(\eta_1, \eta_2) \propto (1, 0)$ or $(0, 1)$ is realized for a positive b, while the double-q phase with $(\eta_1, \eta_2) \propto (1, 1)$ is stabilized for a negative b. We choose the parameter $c_2(N) = 0.01$ in the following part and investigate the magnetic phase diagram for various b.

We determine the magnetic phase by minimizing the Ginzburg-Landau free energy (eq.(1)) with respect to the order parameters η_1 and η_2 and their momentum $\vec{q}_1$ and $\vec{q}_2$ for each temperature T and FFLO wave vector $\vec{q}_{\rm FFLO}$. We assume $\eta_1 \geq \eta_2 \geq 0$ without any loss of the generality. As for the direction of $\vec{q}_{\rm FFLO}$, we assume $\vec{q}_{\rm FFLO} = q_{\rm FFLO}\hat{x}$ for $\vec{H} \parallel [100]$ as in Refs. 27 and 35. Then, the phase diagram is determined by the renormalized parameters $T/T_{\rm N}^0$ and $\xi_{\rm AF}q_0$, where the parameter q_0 describes the mismatch of the higher harmonic FFLO wave vector $2N\vec{q}_{\rm FFLO}$ and the incommensurability along the $\hat{x}$-axis $\vec{q}_{\rm inc}^{(1)} - \vec{q}_{\rm inc}^{(2)}$. We define q_0 as $\vec{q}_{\rm inc}^{(1)} - \vec{q}_{\rm inc}^{(2)} + 2q_0\hat{x} = (2q_{\rm inc} + 2q_0)\hat{x} = 2N\vec{q}_{\rm FFLO}$ with $q_{\rm inc} = 0.125\pi$. Note that $q_0 = 0$ when the commensurate condition $\vec{q}_{\rm inc}^{(1)} - \vec{q}_{\rm inc}^{(2)} = 2N\vec{q}_{\rm FFLO}$ is satisfied. Since the FFLO wave number $q_{\rm FFLO}$ increases with increasing the magnetic field and/or decreasing the temperature,[5] the parameter q_0 increases with the magnetic field, and change its sign at the commensurate line in the H-T phase diagram on which the commensurate condition is satisfied.

We find that three magnetic phases are stabilized. One is the single-q phase where

$$\eta_1 > \eta_2, \quad (3)$$

$$\vec{q}_1 = \vec{q}_{\rm inc}^{(1)} + (1-x)q_0\hat{x}, \quad (4)$$

$$\vec{q}_2 = \vec{q}_{\rm inc}^{(2)} - (1+x)q_0\hat{x}. \quad (5)$$

The mirror symmetry with respect to the x- and y-axes is spontaneously broken in the single-q phase. The others are the double-q phase and double-q' phase where

$$\eta_1 = \eta_2, \quad (6)$$

$$\vec{q}_1 = \vec{q}_{\rm inc}^{(1)} + q_0\hat{x}, \tag{7}$$

$$\vec{q}_2 = \vec{q}_{\rm inc}^{(2)} - q_0\hat{x}, \tag{8}$$

and

$$\eta_1 = \eta_2, \tag{9}$$

$$\vec{q}_1 = \vec{q}_{\rm inc}^{(1)}, \tag{10}$$

$$\vec{q}_2 = \vec{q}_{\rm inc}^{(2)}, \tag{11}$$

respectively.

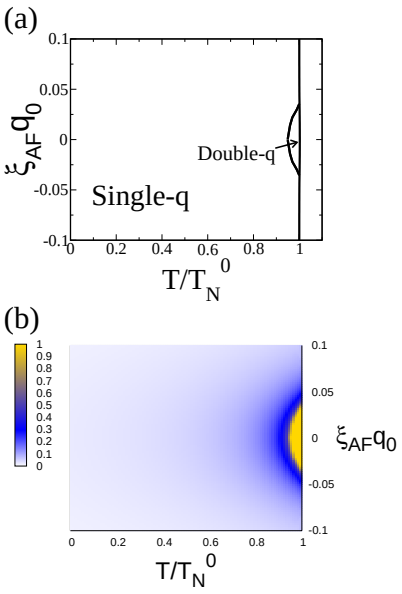

Fig. 1. (Color online) (a) Phase diagram of the Ginzburg-Landau model with $b = 0.1$ for $\xi_{\rm AF}q_0$ and the renormalized temperature $T/T_{\rm N}^0$. The definition of q_0 is given in the text. The q_0 increases with the magnetic field. (b) The ratio of order parameters η_1/η_2.

The analysis of the quadratic terms in eq.(1) shows that the double-q phase is stabilized immediately below the Néel temperature for $(\xi_{\rm AF}q_0)^2 \leq c_2(N)/8$, while a single-$q$ phase is stabilized for $(\xi_{\rm AF}q_0)^2 > c_2(N)/8$. The Néel temperature is increased around the commensurate line $\xi_{\rm AF}q_0 = 0$ owing to the broken translation symmetry. However, the enhancement of the Néel temperature $T_{\rm N} - T_{\rm N}^0 = \frac{c_2(N)}{4}T_{\rm N}^0$ is negligible unless the coupling constant $c_2(N)$ is large.

Figures 1(a)-4(a) show the phase diagram obtained by the numerical calculation for various coupling constants b, while Figs. 1(b)-4(b) show the ratio η_1/η_2. First, we discuss the magnetic phases for a positive b. We see that the single-q phase is stable at low temperatures in Figs. 1 and 2. This is because the quartic term $b\eta_1^2\eta_2^2$ favors the single-q phase. Figure 1 shows that the phase diagram is mostly covered by the single-q phase for a large coupling constant $b \gg c_2(N)$. Then, the double-q phase appears around the Néel temperature when $|\xi_{\rm AF}q_0| \leq \sqrt{c_2(N)/8}$, but it disappears by decreasing the temperature. The double-q phase is stabilized in the intermediate temperature region $T \sim 0.5T_{\rm N}$ for a small and positive

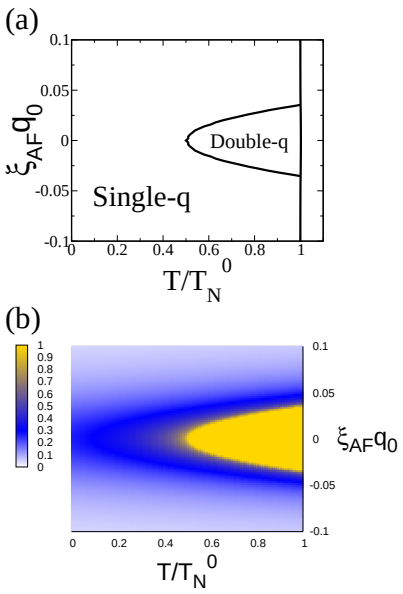

Fig. 2. (Color online) (a) Phase diagram and (b) the ratio of order parameters η_1/η_2 for $b = 0.01$.

$b = c_2(N)$ (Fig. 2). Figures 1(b) and 2(b) show the ratio η_2/η_1 decreases in the single-q phase with decreasing temperature T/T_N^0 and/or increasing the mismatch $|\xi_{\rm AF}q_0|$. The phase transition between the single-q and double-q phases is second order.

Next, we discuss the magnetic phases for a negative coupling constant b. Figures 3(a) and 4(a) show that the double-q phase is stable at low temperatures for $|\xi_{\rm AF}q_0| \leq \sqrt{c_2(N)/4}$ while the double-q' phase is stabilized when the mismatch is larger than the critical value $|\xi_{\rm AF}q_0| > \sqrt{c_2(N)/4}$. The single-$q$ phase appears around the Néel temperature near $|\xi_{\rm AF}q_0| = \sqrt{c_2(N)/4}$. It is shown that the phase diagram is mostly covered by the double-q and double-q' phases. The phase transition is first order between the double-q' phase and the other phases, while that from the double-q phase to the single-q phase is still second order.

In order to understand the magnetic phase diagram more clearly, we plot the $\xi_{\rm AF}q_0$ dependence of order parameters for $b = 0.1$ in Figs. 5(a)-5(c) and that for $b = -0.01$ in Figs. 5(d)-5(f). It is shown that the magnetic phases are almost independent of b around the Néel temperature (Figs. 5(c) and 5(f)), while the single-q phase (double-q or double-q' phase) is stable at low temperatures for the positive (negative) coupling constant b. Fig. 5(e) shows a discontinuous jump of order parameters at the first order transition from the single-q phase to the double-q' phase.

4. High Field Phase Diagram of $CeCoIn_5$

We discuss the possible AFM-FFLO state of $CeCoIn_5$ on the basis of the Ginzburg-Landau theory given in this paper. For this purpose, we show the schematic phase diagram of $CeCoIn_5$ for the magnetic field and temperature in Fig. 6.

The maximum amplitude of the FFLO modulation

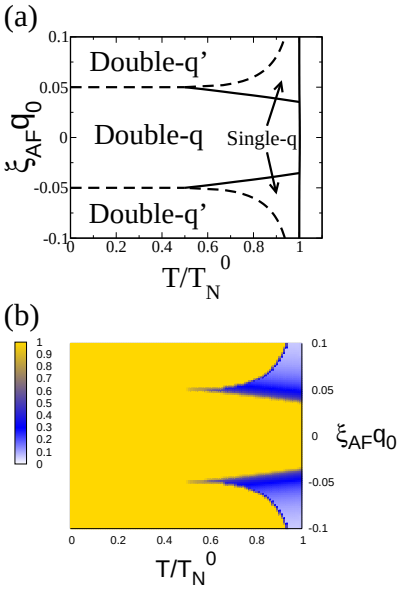

Fig. 3. (Color online) (a) Phase diagram and (b) the ratio of order parameters η_1/η_2 for $b = -0.01$. The dashed lines in (a) show the first order phase transition.

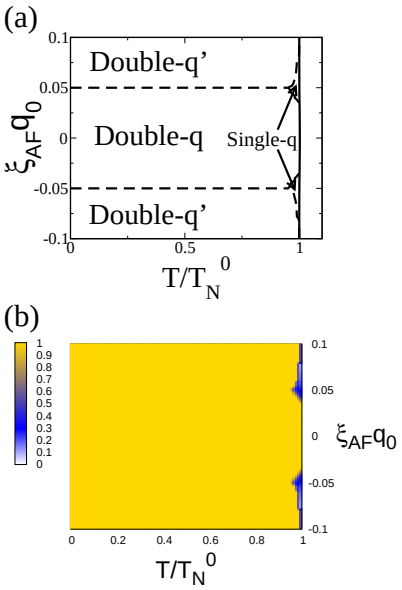

Fig. 4. (Color online) (a) Phase diagram and (b) the ratio of order parameters η_1/η_2 for $b = -0.1$. The dashed lines in (a) show the first order phase transition.

vector $q_{\rm FFLO}$ is approximately the inverse coherence length $q_{\rm FFLO} \sim 1/\xi$. According to the experimental estimation of the coherence length of the superconductivity ξ,[17] the minimum number of N which satisfies the commensurate condition $\vec{q}_{\rm inc}^{(1)} - \vec{q}_{\rm inc}^{(2)} = 2N\vec{q}_{\rm FFLO}$ is approximately obtained as $N \sim 4$. Then, the commensurate condition is satisfied in the FFLO state on a sequence of commensurate lines (dashed lines in Fig. 6) with $N = 4, 5, 6, 7$.....

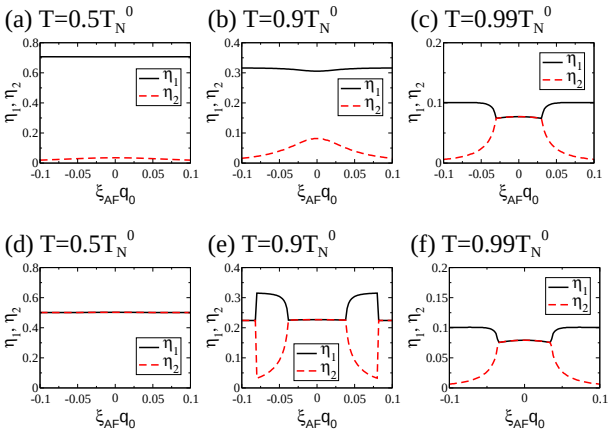

Fig. 5. (Color online) $\xi_{\rm AF}q_0$ dependences of the order parameters η_1 and η_2 for $b = 0.1$ (Figs. 5(a)-5(c)) and $b = -0.01$ (Figs. 5(d)-5(f)). $T = 0.5T_{\rm N}^0$ in Figs. 5(a) and 5(d), $T = 0.9T_{\rm N}^0$ in Figs. 5(b) and 5(e), and $T = 0.99T_{\rm N}^0$ in Figs. 5(c) and 5(f), respectively.

The magnetic phase diagram in the FFLO state is quite different between the positive and negative coupling constants b, as shown in Figs. 6(a) and 6(b). Figure 6(a) shows the phase diagram for a positive b. We see that the AFM-FFLO state is mostly the single-q phase while the double-q phase is stabilized around the AFM transition line near the commensurate lines (shaded area of Fig. 6(a)). Note that the double-q phase does not appear around the first order normal-to-FFLO transition line at which the AFM moment as well as the superconducting order parameter are discontinuous. Since it is expected that the coupling constant $c_2(N)$ decreases with increasing N, the double-q phase is suppressed with decreasing the magnetic field.

Figure 6(b) shows a schematic phase diagram for a negative coupling constant b, where the double-q and double-q' phases are stable at low temperatures. In contrast to Fig. 6(a), a sequence of discontinuous first order transition lines appear in the AFM-FFLO state. These first order transitions occur due to the pinning of AFM moment on the FFLO nodal planes. This is a direct consequence of the broken translation symmetry in the inhomogeneous Larkin-Ovchinnikov state. However, these first order transitions have not been observed in the experiments of $CeCoIn_5$. This indicates that the coupling constant b is positive in $CeCoIn_5$. Thus, the phase diagram in Fig. 6(a) is more likely realized in $CeCoIn_5$ than Fig. 6(b). Since the second order phase transition shown in Fig. 2 has not been observed in the magnetic phase of $CeCoIn_5$, The coupling constant b should be much larger than $c_2(n)$. Then, the AFM-FFLO state is mostly covered by the single-q phase where the mirror symmetry with respect to the x- and y-axis is broken. It is desirable that the phase diagram of $CeCoIn_5$ will be investigated by the intensive experiments in the magnetic field along [100] axis.

The phase diagram in Fig. 6(a) is supported by the nuclear magnetic resonance (NMR) and neutron scattering measurements for $CeCoIn_5$. We first discuss the neutron scattering measurement. According to the results

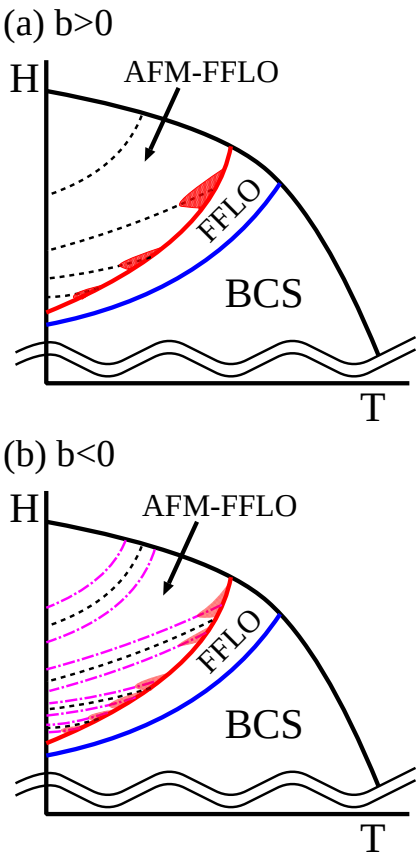

Fig. 6. (Color online) Schematic phase diagram of $CeCoIn_5$ for the magnetic field along [100] direction. (a) $b > 0$ and (b) $b < 0$. "BCS", "FFLO", and "AFM-FFLO" states are shown in the figure. The dashed lines show the commensurate lines where the commensurate condition is satisfied. The shaded region shows the double-q phase in (a), while it shows the single-q phase in (b). The dash-dotted lines in (b) show the first order phase transition lines between the double-q phase and double-q' phase.

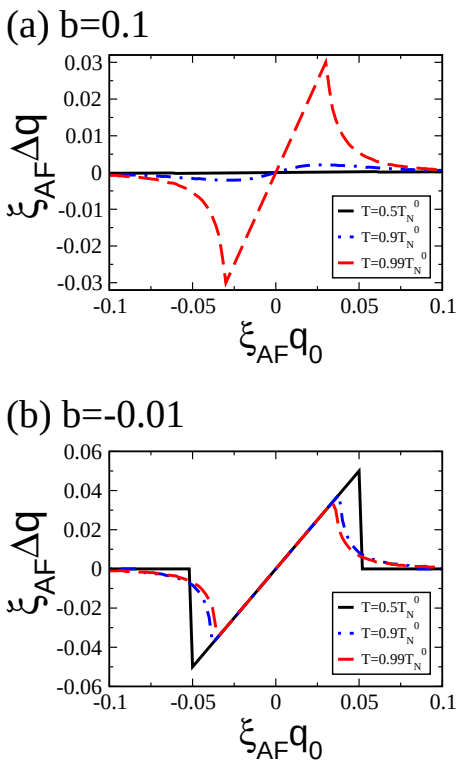

Fig. 7. (Color online) The shift of the position of main Bragg peak from $\vec{q}_{\rm inc}^{(1)}$. We plot $\xi_{\rm AF}\Delta q$ for $T = 0.5T_{\rm N}^0$, $T = 0.9T_{\rm N}^0$, and $T = 0.99T_{\rm N}^0$, where Δq is defined by $\Delta q\hat{x} = \vec{q}_1 - \vec{q}_{\rm inc}^{(1)}$.

obtained by Kenzelmann *et al.*,, the position of Bragg peaks does not change with increasing the magnetic field along [100] direction.[24] The phase diagram for a negative b (Figs. 3 and 4) is incompatible with this experimental result. Figure 7 shows the $\xi_{\rm AF}q_0$ dependence of the shift of main Bragg peak $\Delta q\hat{x} = \vec{q}_1 - \vec{q}_{\rm inc}^{(1)}$. For $b < 0$, Fig. 7(b) shows the shift $\xi_{\rm AF}\Delta q > 0.05$ at low temperatures. When we assume $\xi_{\rm AF} = 3$, $\Delta q \sim 0.006\pi$ near the first order transition lines. This shift is larger than the experimental error,[24] and therefore can be observed if it would occur. However, the experimental result has not shown the shift of Bragg peaks.

On the other hand, the neutron scattering measurement is consistent with our results for the positive b. Fig. 7(a) shows a pronounced shift $\xi_{\rm AF}\Delta q$ up to 0.03 near the Néel temperature, but the shift rapidly decreases with decreasing the temperature. Since the magnetic moment is tiny near the AFM transition, it is difficult to experimentally observe of the shift of Bragg peaks around $T_{\rm N}$. Thus, our results in Fig. 7(a) are consistent with the experimental observation.[24]

We here comment on the effect of domain structure in the single-q phase. For the magnetic field along [100] direction the elastic Bragg peaks appear at $\vec{Q} = \vec{Q}_0 \pm \vec{q}_{\rm inc}^{(1)}$ as well as at its symmetric point $\vec{Q} = \vec{Q}_0 \pm \vec{q}_{\rm inc}^{(2)}$.[23,24] This result seems to be incompatible with the phase diagram for $b > 0$, because the intensity of Bragg peaks at $\vec{Q} = \vec{Q}_0 \pm \vec{q}_{\rm inc}^{(2)}$ is very weak in the single-q phase with $|\eta_1| \gg |\eta_2|$. However, the observed four Bragg peaks are consistent with the single-q phase by taking into account the domain formation of two degenerate single-q states, i.e. $|\eta_1| > |\eta_2|$ and $|\eta_1| < |\eta_2|$.

The phase diagram in Fig. 6(a) is also supported by the NMR measurements which can distinguish the single-q phase from the double-q phase. When the hyperfine coupling has the dipolar symmetry, the NMR spectrum at the In(2b) site shows the distribution function of the internal field arising from the AFM staggered moment.[36] The experimental results show the double peak structure of NMR spectrum at the In(2b) site.[16,22,37–39] According to our analysis which will be published elsewhere, these results are consistent with the single-q phase, but not with the double-q phase. Thus, both neutron scattering and NMR measurements support the positive coupling constant b (Figs. 1 and 6(a)) and rule out the negative b (Figs. 3, 4 and 6(b)).

When we take into account the broken translation symmetry arising from the vortex lattice, other commensurate lines can appear in the phase diagram and stabilize the double-q phase around $T = T_{\rm N}$. However, it is expected that the effect of vortex lattice on the magnetic order is smaller than that of the FFLO nodal planes when the Maki parameter is large enough to make the

lattice spacing of vortices much larger than the coherence length.

5. Summary

We investigated the incommensurate AFM order in the FFLO superconducting state with a particular interest on the possible coexistence of the AFM order and FFLO superconductivity in the HFSC phase of $CeCoIn_5$. Assuming the incommensurate AFM order with $\vec{q}_{\rm inc} \parallel [110]$ or $\vec{q}_{\rm inc} \parallel [1\bar{1}0]$, we examined the magnetic phase in the magnetic field along [100] direction. We find that the multiple AFM phases appear in the H-T phase diagram owing to the broken translation symmetry in the FFLO superconducting state. The comparison between the Ginzburg-Landau theory and experimental results shows that the AFM-FFLO state is mostly covered by the single-q phase in which the mirror symmetry with respect to the x and y axes is broken.

Acknowledgements

The authors are grateful to D.F. Agterberg, S. Gerber, R. Ikeda, M. Kenzelmann, K. Kumagai, K. Machida, Y. Matsuda, V. F. Mitrović, and H. Tsunetsugu for fruitful discussions. This work was supported by a Grant-in-Aid for Scientific Research on Innovative Areas "Heavy Electrons" (No. 21102506) from MEXT, Japan. It was also supported by a Grant-in-Aid for Young Scientists (B) (No. 20740187) from JSPS. Numerical computation in this work was carried out at the Yukawa Institute Computer Facility. YY is grateful for the hospitality of the Pauli Center of ETH Zurich. This work was also supported by the Swiss Nationalfonds and the NCCR MaNEP.

1) P. Fulde and R. A. Ferrell: Phys. Rev. **135** (1964) A550.
2) A. I. Larkin and Y. N. Ovchinnikov: Sov. Phys. JETP **20** (1965) 762.
3) H. A. Radovan, N. A. Fortune, T. P. Murphy, S. T. Hannahs, E. C. Palm, S. W. Tozer, and D. Hall: Nature **425** (2003) 51.
4) A. Bianchi, R. Movshovich, C. Capan, P. G. Pagliuso, and J. L. Sarrao: Phys. Rev. Lett. **91** (2003) 187004.
5) Y. Matsuda and H. Shimahara: J. Phys. Soc. Jpn. **76** (2007) 051005.
6) S. Uji, T. Terashima, M. Nishimura, Y. Takahide, T. Konoike, K. Enomoto, H. Cui, H. Kobayashi, A. Kobayashi, H. Tanaka, M. Tokumoto, E. S. Choi, T. Tokumoto, D. Graf, and J. S. Brooks: Phys. Rev. Lett. **97** (2006) 157001.
7) J. Singleton, J. A. Symington, M.-S. Nam, A. Ardavan, M. Kurmoo, and P. Day: J. Phys.: Condens. Matter **12** (2000) L641.
8) R. Lortz, Y. Wang, A. Demuer, P. H. M. Böttger, B. Bergk, G. Zwicknagl, Y. Nakazawa, and J. Wosnitza: Phys. Rev. Lett. **99** (2007) 187002.
9) J. Shinagawa, Y. Kurosaki, F. Zhang, C. Parker, S. E. Brown, D. Jérome, J. B. Christensen, and K. Bechgaard: Phys. Rev. Lett. **98** (2007) 147002.
10) G. B. Partridge, W. Li, R. I. Kamar, Y.-A. Liao, and R. G. Hulet: Science **311** (2006) 503.
11) M. W. Zwierlein, A. Schirotzek, C. H. Schunck, and W. Ketterle: Science **311** (2006) 492.
12) R. Casalbuoni and G. Nardulli: Rev. Mod. Phys. **76** (2004) 263.
13) T. Watanabe, Y. Kasahara, K. Izawa, T. Sakakibara, Y. Matsuda, C. J. van der Beek, T. Hanaguri, H. Shishido, R. Settai, and Y. Onuki: Phys. Rev. B **70** (2004) 020506.
14) C. Capan, A. Bianchi, R. Movshovich, A. D. Christianson, A. Malinowski, M. F. Hundley, A. Lacerda, P. G. Pagliuso, and J. L. Sarrao: Phys. Rev. B **70** (2004) 134513.
15) C. Martin, C. C. Agosta, S. W. Tozer, H. A. Radovan, E. C. Palm, T. P. Murphy, and J. L. Sarrao: Phys. Rev. B **71** (2005) 020503.
16) V. F. Mitrović, M. Horvatić, C. Berthier, G. Knebel, G. Lapertot, and J. Flouquet: Phys. Rev. Lett. **97** (2006) 117002.
17) C. F. Miclea, M. Nicklas, D. Parker, K. Maki, J. L. Sarrao, J. D. Thompson, G. Sparn, and F. Steglich: Phys. Rev. Lett. **96** (2006) 117001.
18) V. F. Correa, T. P. Murphy, C. Martin, K. M. Purcell, E. C. Palm, G. M. Schmiedeshoff, J. C. Cooley, and S. W. Tozer: Phys. Rev. Lett. **98** (2007) 087001.
19) H. Adachi and R. Ikeda: Phys. Rev. B **68** (2003) 184510.
20) R. Ikeda: Phys. Rev. B **76** (2007) 134504.
21) R. Ikeda: Phys. Rev. B **76** (2007) 054517.
22) B.-L. Young, R. R. Urbano, N. J. Curro, J. D. Thompson, J. L. Sarrao, A. B. Vorontsov, and M. J. Graf: Phys. Rev. Lett. **98** (2007) 036402.
23) M. Kenzelmann, T. Strassle, C. Niedermayer, M. Sigrist, B. Padmanabhan, M. Zolliker, A. D. Bianchi, R. Movshovich, E. D. Bauer, J. L. Sarrao, and J. D. Thompson: Science **321** (2008) 1652.
24) M. Kenzelmann, S. Gerber, N. Egetenmeyer, J. L. Gavilano, T. Strässle, A. D. Bianchi, E. Ressouche, R. Movshovich, E. D. Bauer, J. L. Sarrao, and J. D. Thompson: Phys. Rev. Lett. **104** (2010) 127001.
25) Y. Kitaoka, S. Kawasaki, T. Mito, and Y. Kawasaki: J. Phys. Soc. Jpn. **74** (2005) 186.
26) Y. Yanase and M. Sigrist: J. Phys.: Conf. Ser. **150** (2009) 052287.
27) Y. Yanase and M. Sigrist: J. Phys. Soc. Jpn. **78** (2009) 114715.
28) K. Miyake: J. Phys. Soc. Jpn. **77** (2008) 123703.
29) A. Aperis, G. Varelogiannis, P. B. Littlewood, and B. D. Simons: J. Phys.: Condens. Matter **20** (2008) 434235.
30) A. Aperis, G. Varelogiannis, and P. B. Littlewood: Phys. Rev. Lett. **104** (2010) 216403.
31) D. F. Agterberg, M. Sigrist, and H. Tsunetsugu: Phys. Rev. Lett. **102** (2009) 207004.
32) R. Ikeda, Y. Hatakeyama, and K. Aoyama: Phys. Rev. B **82** (2010) 060510.
33) A. Bianchi, R. Movshovich, I. Vekhter, P. G. Pagliuso, and J. L. Sarrao: Phys. Rev. Lett. **91** (2003) 257001.
34) F. Ronning, C. Capan, A. Bianchi, R. Movshovich, A. Lacerda, M. F. Hundley, J. D. Thompson, P. G. Pagliuso, and J. L. Sarrao: Phys. Rev. B **71** (2005) 104528.
35) Y. Yanase and M. Sigrist: J. Phys.: Condens. Matter **23** (2010) 094219.
36) N. J. Curro, B.-L. Young, R. R. Urbano, and M. J. Graf: arXiv:0908.0565; arXiv:0910.0288 (2009) .
37) G. Koutroulakis, V. F. Mitrović, M. Horvatić, C. Berthier, G. Lapertot, and J. Flouquet: Phys. Rev. Lett. **101** (2008) 047004.
38) G. Koutroulakis, M. D. Stewart, V. F. Mitrović, M. Horvatić, C. Berthier, G. Lapertot, and J. Flouquet: Phys. Rev. Lett. **104** (2010) 087001.
39) K. Kumagai, H. Shishido, T. Shibauchi, and Y. Matsuda: Phys. Rev. Lett. **106** (2011) 137004.